



Cite this: *Soft Matter*, 2023, 19, 743

## Regulation of the nanostructures self-assembled from an amphiphilic azobenzene homopolymer: influence of initial concentration and solvent solubility parameter†

Hui Sun, \*<sup>a</sup> Ying Leng,<sup>a</sup> Xiaoyan Zhou,<sup>a</sup> Xiao Li<sup>a</sup> and Tian Wang<sup>b</sup>

The control over the morphology and nanostructure of soft nanomaterials self-assembled from amphiphilic polymers is of high interest, but is still challenging. Herein, we manipulate the morphology of bowl-shaped nanoparticles by changing initial polymer concentrations, and prepare nanotubes and nanowires, both twisted and not, by using solvents with different solubility parameters. An amphiphilic azobenzene homopolymer (poly(4-(phenyldiazenyl)phenyl methacrylamide), PAzoMAA) is designed and synthesized *via* reversible addition fragmentation chain transfer (RAFT) polymerization, which can self-assemble into bowl-shaped nanoparticles promoted by the synergy of hydrogen bonding and  $\pi$ - $\pi$  interaction. More significantly, the opening size of the bowl-shaped nanoparticles can be controlled by changing initial polymer concentrations. Nanotubes and nanowires, both twisted and not, are also obtained using a solvothermal method in alcohols. The relationship between the structure of the nanomaterials and the solubility parameters of the alcohols is investigated, revealing the molecular arrangement patterns of PAzoMAA in different nanostructures. Overall, we propose a facile strategy to manipulate the microstructure of bowl-shaped nanoparticles and one-dimensional nanomaterials by adjusting initial polymer concentration and solvent solubility parameters. Our study may bring new avenues for controlling the nanostructures of soft nanomaterials.

Received 5th August 2022,  
Accepted 26th December 2022

DOI: 10.1039/d2sm01059c

[rsc.li/soft-matter-journal](http://rsc.li/soft-matter-journal)

## Introduction

The control of the morphology and microstructures of soft nanomaterials prepared by the self-assembly of amphiphilic polymers has always been the focus in the field of macromolecular self-assembly.<sup>1–4</sup> Physicochemical properties, such as rheological, optical and physiological properties,<sup>5–7</sup> are affected by the shape and morphology of nanomaterials. This allows for their application in drug delivery,<sup>8</sup> catalysis,<sup>9</sup> antimicrobial agents<sup>10</sup> and imaging,<sup>11</sup> among others.<sup>12–16</sup> There are several strategies to manipulate the morphology of soft nanomaterials, either during or post self-assembly.<sup>17–20</sup> For instance, regulation of the self-assembly conditions including solvent,<sup>21,22</sup> temperature,<sup>23</sup> pH,<sup>24</sup> concentration,<sup>25,26</sup> *etc.* have been widely used to control the shape, size, and microstructure

of the assemblies. In addition, post self-assembly methods such as stimuli-responsive shape transformation,<sup>27,28</sup> hierarchical self-assembly,<sup>29,30</sup> and particle fusion<sup>31–33</sup> also allow the controlling over the microstructure of soft nanomaterials.

Bowl-shaped nanoparticles are asymmetric hollow structures with an interior hole and a large opening on the surface. The pioneering study of preparation of nanobowls by polymer self-assembly was reported by Eisenberg and coworkers.<sup>34</sup> Later, they proposed an additional viscosity-control mechanism to explain the formation of bowl-shaped nanoparticles.<sup>35</sup> Recently, our group prepared nanobowls with controlled openings and interior holes by changing the molecular weight of amphiphilic homopolymers and captured the intermediates during the formation of nanobowls.<sup>36</sup> Despite the previous studies, the controlling over the opening size of nanobowls by self-assembly parameters such as polymer concentration is an important contribution to this field.

The solubility parameter ( $\delta$ ) is crucial for determining the interactions between polymers and solvents. Typically, if the solubility parameters of the polymer and solvent are too similar, or equal, the polymer can dissolve in the solvent.<sup>37</sup> The solubility parameter of solvent also influences the self-assembly behaviour of amphiphilic polymers, altering the

<sup>a</sup> School of Chemistry and Chemical Engineering, State Key Laboratory of High-Efficiency Coal Utilization and Green Chemical Engineering, Ningxia University, Yinchuan, 750021, China. E-mail: sunhui@nxu.edu.cn

<sup>b</sup> Department of Chemistry, University of Washington, Seattle, WA, 98195, USA

† Electronic supplementary information (ESI) available: Characterizations, synthetic routes, calculation of the molecular length and solubility parameter of PAzoMAA, NMR, DSC, GPC, DLS, Zeta potential, UV-vis, SEM and TEM. See DOI: <https://doi.org/10.1039/d2sm01059c>

morphology and structure of the obtained nanomaterials.<sup>38,39</sup> For instance, Shen and coworkers investigated the influence of the solubility parameter of mixed solvents on the formation of cubosomes or hexasomes self-assembled from a rod-coil polymer.<sup>40</sup> Du *et al.* revealed the evolution of diverse higher-order membrane structures of block copolymer vesicles from the perspective of the co-solvent solubility parameter.<sup>41</sup> Recently, they found that a higher solubility parameter of the mixed solvents was favourable for the formation of tetrapod polymersomes and micelle clusters.<sup>42</sup> Therefore, the solubility parameter of the solvent has a critical impact on the morphology, size and microstructure of the formed nanomaterials. However, most previous studies merely focused on the influence of the solvent solubility parameters on the self-assembly behaviour of amphiphilic polymers quantitatively.<sup>41,43–45</sup> Consequently, the relationship between the morphology of the nanomaterials and the solubility parameter of the solvents is unclear since the solubility parameters of polymers vary greatly.

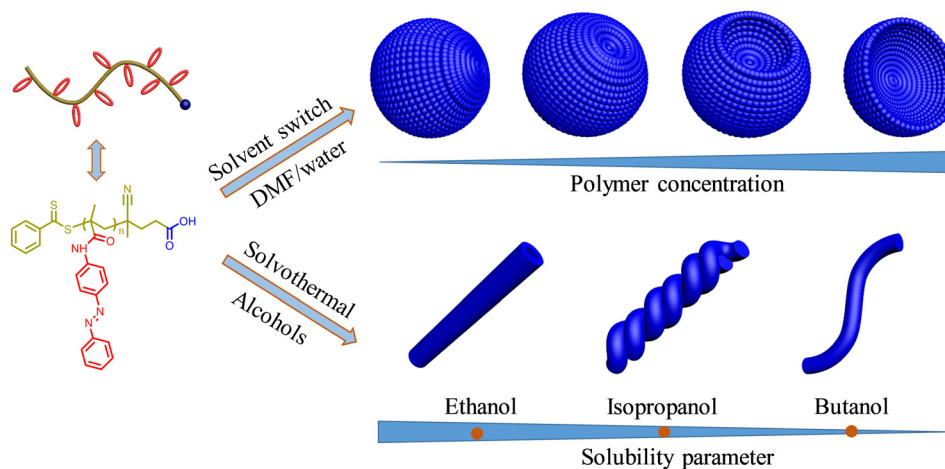
Herein, we controlled the morphology of bowl-shaped nanoparticles by changing polymer concentrations and revealed the relationship between the microstructure of one dimensional nanomaterials and the difference in solubility parameters of the polymer and solvents. As shown in Scheme 1, in very dilute solution ( $0.05 \text{ mg mL}^{-1}$ ), compound micelles were formed. With the increase of polymer concentration, bowl-shaped nanoparticles with controlled opening sizes were obtained. Due to the increase of polymer concentration, the local density of polymer chains increases, leading to the enhanced intermolecular interaction including hydrogen bonding and  $\pi$ - $\pi$  interaction. Therefore, the local viscosity inside the preformed spheres increases during self-assembly, which hinders the homogeneous shrinkage of the preformed spheres, resulting in the formation of surface holes and nanobowls with large openings.<sup>35,36</sup> Different from our previous studies,<sup>36,46</sup> we found that there were actually two stages for the formation of bowl-shaped nanoparticles with increased opening sizes, *i.e.* broken and collapse of the thinner part of the preformed

hollow spheres. In addition, we calculated the solubility parameter of PAzoMAA and investigated the influence of solubility parameter of the solvents on the microstructure of the assemblies in alcohols. We discovered that a suitable difference in solubility parameters facilitated the regular arrangement of polymer chains, leading to the formation of nanotubes, while small difference in solubility parameters promoted the formation of nanowires, both twisted and not.

## Results and discussion

The PAzoMAA homopolymer was synthesized *via* RAFT polymerization of 4-(phenyldiazenyl)phenyl methacrylamide (AzoMAA) with 4-cyano-4-((phenylcarbonothioyl)thio)pentanoic acid (CPAD) as chain transfer agent. The synthetic route of AzoMAA monomer and PAzoMAA was illustrated in Scheme S1 (ESI<sup>†</sup>). The nuclear magnetic resonance (NMR) in Fig. S1 and S2 (ESI<sup>†</sup>) demonstrated the successful synthesis of the monomer and homopolymer. And the disappearance of the signal of the double bond in Fig. S2 (ESI<sup>†</sup>) confirmed the entire consumption of the monomer, corresponding to a degree of polymerization (DP) of 26. The gel permeation chromatography (GPC) trace in Fig. S3 (ESI<sup>†</sup>) revealed a molecular weight of 4700 Da with a low polydispersity index ( $\mathcal{D}$ ) of 1.21. In addition, the glass transition temperature ( $T_g$ ) of the PAzoMAA was  $75.2 \text{ }^\circ\text{C}$  without endothermic and exothermic peaks, as confirmed by differential scanning calorimetry (DSC) curve in Fig. S4 (ESI<sup>†</sup>).

Previous studies demonstrated that additional viscosity provided by non-covalent interactions such as hydrogen bonding and  $\pi$ - $\pi$  interaction could promote the formation of bowl-shaped nanoparticles.<sup>35,36</sup> Therefore, we introduced azobenzene group and amide bond at the side chain of PAzoMAA to afford  $\pi$ - $\pi$  stacking and hydrogen bonding interaction (Scheme 1), respectively.<sup>47</sup> Indeed, bowl-shaped nanoparticles with different opening sizes were prepared, as shown in Fig. 1. The obvious red shift of the adsorption peak of azobenzene in



**Scheme 1** Fabrication of bowl-shaped nanoparticles with controlled opening sizes by changing polymer concentration, and the impact of alcohols with various solubility parameters on the morphology of one-dimensional nanomaterials.

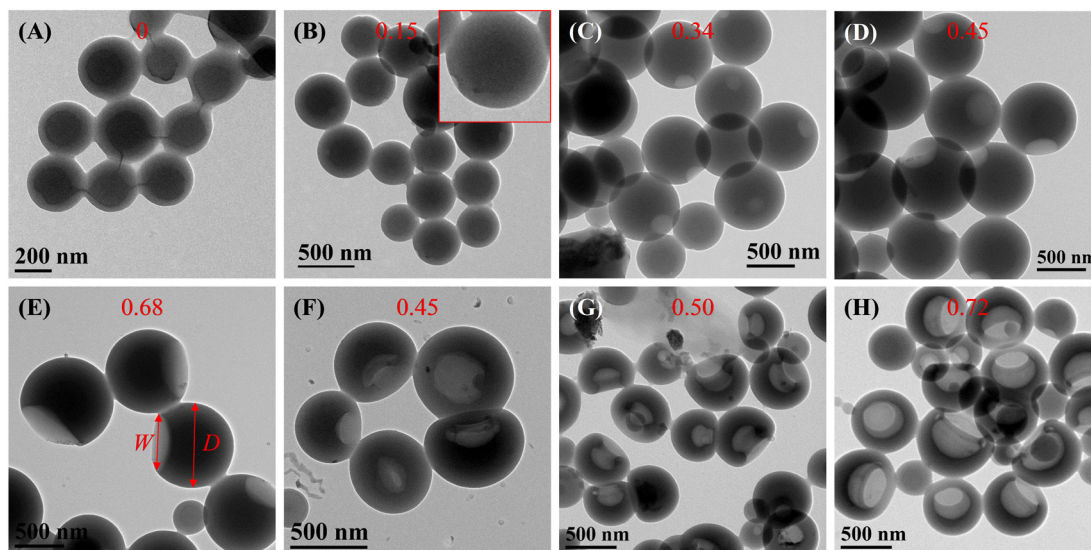


**Fig. 1** TEM images of (A) compound micelles and (B–H) bowl-shaped nanoparticles with different opening sizes. The inserted texts are the ratios of the width to the diameter ( $W/D$ ) of the bowl-shaped nanoparticles. The initial concentrations of (A–H) are 0.05, 0.1, 0.2, 0.4, 0.5, 0.6, 0.8, 1.0  $\text{mg mL}^{-1}$ , respectively.

Fig. S5 (ESI<sup>†</sup>) confirmed the strong  $\pi$ - $\pi$  interaction during self-assembly. When the initial concentration was low ( $0.05 \text{ mg mL}^{-1}$ ), compound micelles with diameter of  $310 \pm 48 \text{ nm}$  were formed due to the low local viscosity, which could not hinder the homogeneous shrinkage of the preformed spheres (Fig. 1A).<sup>35,36,47</sup> As for the formation of bowl-shaped nanoparticles, the size of the openings continuously increased with the increase of polymer concentration (Fig. 1B–H). In order to reduce the polydispersity of the obtained bowl-shaped nanoparticles, we decreased the drop rate of deionized water to  $2 \text{ mL hour}^{-1}$ . As expected, the bowl-shaped nanoparticles showed narrower size distribution of  $770 \pm 43 \text{ nm}$ , which is much smaller than that in Fig. 1D ( $770 \pm 87 \text{ nm}$ ), as shown in Fig. S6 (ESI<sup>†</sup>). The hydrodynamic diameters of the compound micelles and bowl-shaped nanoparticles were presented in Fig. S7 (ESI<sup>†</sup>). The strong negative Zeta potential demonstrated that carboxylic groups covered on the surface of bowl-shaped nanoparticles to maintain the colloidal stability (Fig. S8, ESI<sup>†</sup>). Both PAzoMAA and bowl-shaped nanoparticles exhibited UV irradiation induced *trans*-*cis* isomerization (Fig. S9

and S10, ESI<sup>†</sup>). The isomerization reaction of bowl-shaped nanoparticles is much slower than that of PAzoMAA. This phenomenon may be ascribed to the glassy state of the azobenzene groups inside the bowl-shaped nanoparticles, which hinders the isomerization transformation of azobenzene pendants.

In order to quantitatively determine the opening size of bowl-shaped nanoparticles, we defined the ratio of the width ( $W$ ) to diameter ( $D$ ) of the bowl-shaped nanoparticles as  $W/D$ , as shown in red arrows in Fig. 1E and inserted red text in Fig. 1A–H. Theoretically, the value of  $W/D$  should increase with the polymer concentration as the opening size increases due to the enlarged local viscosity. However, there is a decrease of  $W/D$  when the polymer concentration increased from 0.5 to 0.6  $\text{mg mL}^{-1}$ . Therefore, we analysed the relationship between the  $W/D$  and polymer concentration, as shown in Fig. 2A. There is an inflection point of the  $W/D$ . Taking an insight into the TEM images of bowl-shaped nanoparticles, we found that there were two stages for the formation of bowl-shaped nanoparticles with the increase of polymer concentration. When the polymer concentration is

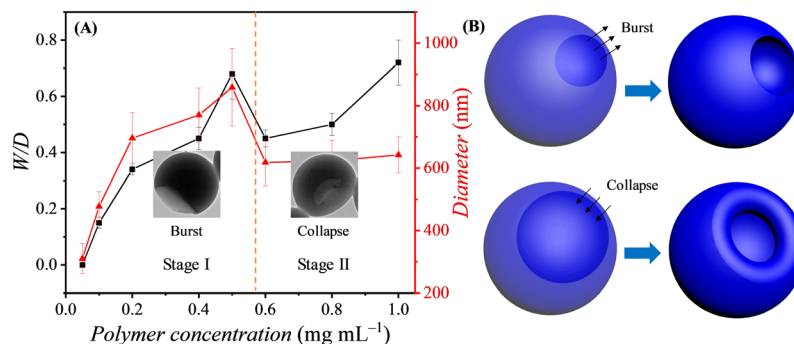


**Fig. 2** (A) Relationship between the diameter and  $W/D$  of bowl-shaped nanoparticles and polymer concentration and (B) schematic illustration of the two stages during the formation of bowl-shaped nanoparticles with increasing opening sizes.

below  $0.5 \text{ mg mL}^{-1}$ , the inner cavity is small and the curvature of the cavity is so large that hinder the collapse of the thinner part of the asymmetric hollow spheres, leading to the burst of the thinner part and the formation of the cavity (Fig. 2B). As the polymer concentration increases to above  $0.5 \text{ mg mL}^{-1}$ , the thinner part of the asymmetric hollow spheres is soft enough to collapse, as shown in the inserted TEM images in Fig. 2A and schematic illustration in Fig. 2B. Though the morphology of bowl-shaped nanoparticles is similar when the polymer concentration is below or above  $0.5 \text{ mg mL}^{-1}$ , the formation mechanism of the cavity is different, which also explains the decrease of the diameter of bowl-shaped nanoparticles at this concentration (Fig. S7, ESI<sup>†</sup>). The TEM images at a polymer concentration of  $0.55 \text{ mg mL}^{-1}$  in Fig. S11 (ESI<sup>†</sup>) and SEM images in Fig. S12 (ESI<sup>†</sup>) further confirmed the statement.

The solubility parameter of solvents has a significant influence on the interaction between polymers and solvents, which determines the solubility and self-assembly behaviour of amphiphilic polymers. Therefore, we investigated the influence of the solubility parameter of solvents on the morphology and microstructure of the nanomaterials self-assembled from PAzoMAA. Firstly, the solubility parameter of the homopolymer was calculated according to Fedors's method.<sup>37</sup> The solubility parameter of PAzoMAA was calculated to be  $24.9 \text{ J}^{1/2} \text{ cm}^{-3/2}$ , as presented in Table S1 (ESI<sup>†</sup>). Alcohols with solubility parameters close to PAzoMAA were chosen as solvents, including ethanol, isopropanol, and butanol with  $\delta$  of 26.3, 23.5 and  $23.3 \text{ J}^{1/2} \text{ cm}^{-3/2}$ , respectively. The PAzoMAA with concentration of  $0.5 \text{ mg mL}^{-1}$  was dispersed in the alcohols. The solution was heated up to  $75 \text{ }^\circ\text{C}$  for 4 hours and cooled naturally to ambient

temperature to induce the self-assembly of PAzoMAA. As shown in Fig. 3A and B, when the solvent is ethanol, nanotubes with uniform diameter were formed. The outer and inner diameters were measured to be 29.2 and 9.5 nm, respectively, as illustrated in Fig. 3C. As the solvent changed to isopropanol, twisted nanowires with single nanowire diameter of 10.1 nm were formed (Fig. 3D–F). Interestingly, when using butanol with slightly smaller  $\delta$  than isopropanol ( $23.3 \text{ J}^{1/2} \text{ cm}^{-3/2}$ ) as solvent, nanowires without twisted structure were observed (Fig. 3G and H). The diameter of the nanowires was similar with that of twisted nanowires in isopropanol (Fig. 3F and I).

In order to determine the diameter distribution of nanotube, nanowires and twisted nanowires, supplementary TEM images with high resolution were provided, as illustrated in Fig. S13 (ESI<sup>†</sup>), showing average diameters of  $29.2 \pm 4.3$ ,  $10.1 \pm 2.2$  and  $10.1 \pm 1.8 \text{ nm}$  of nanotube, nanowires and twisted nanowires, respectively. The thick nanowires are formed by the twining and aggregation of thin nanowires.

To gain deeper insights into the effect of solubility parameter of the solvents on the morphology and microstructure of the formed one-dimensional nanomaterials, the molecular chain arrangement patterns of PAzoMAA in nanotube, nanowires and twisted nanowires were analysed, as proposed in Fig. 4. Firstly, the molecular length of PAzoMAA was calculated to be 4.8 nm, as detailed in the ESI.<sup>†</sup> The wall thickness of the nanotube was measured to be 9.8 nm, which is twice of the molecular length of PAzoMAA. Therefore, we speculated that PAzoMAA arranged in a tail-to-tail parallel manner, as illustrated in Fig. 4. The diameters of the nanowires and twisted nanowires were also twice of the molecular length of

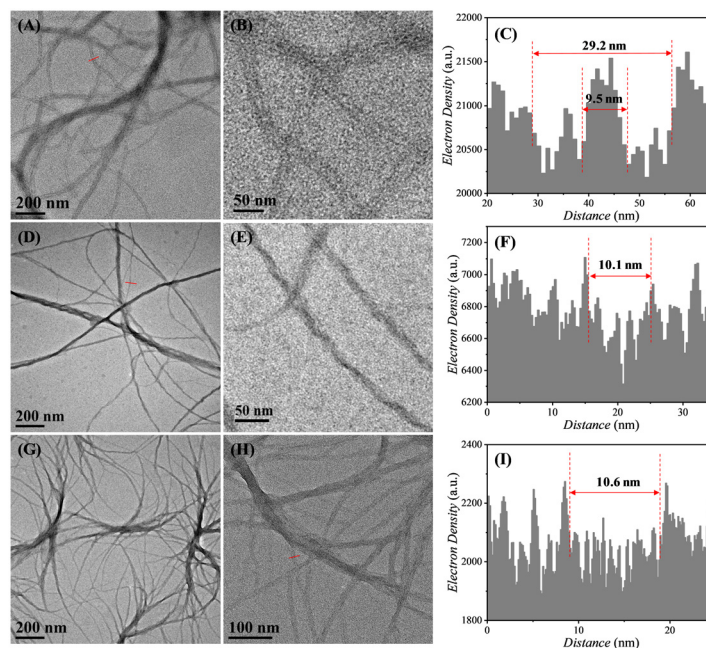


**Fig. 3** TEM images of one-dimensional nanomaterials self-assembled from PAzoMAA in alcohols with different solubility parameters by solvothermal method. (A and B) TEM images of nanotubes formed in ethanol and (C) electron density crossed by the red line in (A); (D and E) TEM images of twisted nanowires formed in isopropanol and (F) electron density crossed by the red line in (D); (G and H) TEM images of nanowires formed in butanol and (I) electron density crossed by the red line in (H).

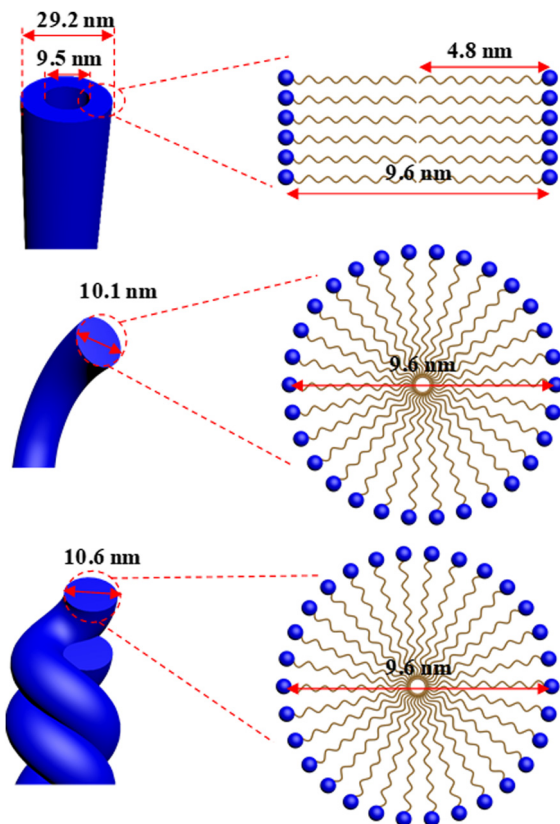


Fig. 4 Proposed arrangement patterns of PAzoMAA chains inside nanotubes, nanowires and twisted nanowires.

PAzoMAA, indicating a circular arrangement of molecular chains with non-polar tails forming the core and polar head forming the shell. The strong negative Zeta potentials of nanotubes ( $-34.4$  mV, Fig. S14, ESI<sup>†</sup>), nanowires ( $-35.1$  mV, Fig. S15, ESI<sup>†</sup>) and twisted nanowires ( $-34.8$  mV, Fig. S16, ESI<sup>†</sup>) further confirmed the hypothesis. Comparing the solubility parameters of ethanol, isopropanol, and butanol, we found that a proper difference between the PAzoMAA and the solvent promoted the regular arrangement of molecular chains. In ethanol, rigid nanotubes were formed, while semi-rigid twisted nanowires and nanowires were obtained in isopropanol and butanol. The fully stretched alignment of *trans*-azobenzene in isopropanol may generate torsional strain, which promotes the formation of twisted nanowires.<sup>48</sup> Though there are strong negative charges on the surface of nanowires, the degree of ionization of carboxylic groups in alcohols may be still low, and the hydrogen bonds between carboxylic groups counteract part of the electrostatic repulsion, facilitating the contact and twining of nanowires.<sup>49</sup> To further prove the speculation, we heated the PAzoMAA solution in butanol to  $100$  °C, which would decrease the solubility parameter of PAzoMAA since the cohesive energy would decrease with increasing temperature.<sup>37</sup> So the solubility parameter of PAzoMAA was closer to that of butanol. As expected, compound micelles instead of one-dimensional nanomaterials were formed (Fig. S17, ESI<sup>†</sup>).

## Conclusions

In summary, we manipulated the morphology and structure of the soft nanomaterials self-assembled from an amphiphilic azobenzene homopolymer by adjusting the polymer concentration and adopting solvents with various solubility parameters. Upon changing polymer concentration, bowl-shaped nanoparticles with controlled opening sizes were prepared. We found that there were two stages during the formation of bowl-shaped nanoparticles with increasing opening sizes, which had never been reported before and was beneficial for understanding the formation mechanism of such asymmetric nanostructures. Furthermore, one-dimensional nanostructures including nanotubes and nanowires, both twisted and not, were fabricated by regulating the solubility parameter of the solvents. It was emphasized that a proper difference of solubility parameter between PAzoMAA and the solvent was favoured for the formation of rigid nanostructures, *e.g.*, nanotubes, while a similar solubility parameter promoted the formation of nanowires and compound micelles.

## Author contributions

Hui Sun: supervision, conceptualization, writing – original draft preparation, writing – reviewing and editing. Ying Leng: data curation, investigation. Xiaoyan Zhou: visualization. Xiao Li: validation. Tian Wang: writing – reviewing and editing.

## Conflicts of interest

There are no conflicts to declare.

## Acknowledgements

This work was supported by Graduate Innovation Program of Ningxia University (CXXM202230), Natural Science Foundation of China (U22A20119) and Natural Science Foundation of Ningxia (2021AAC03026 and 2020AAC03003). H. S. thanks the Ningxia Youth Talent Support Project of Science and Technology and Young Scholars of Western China of CAS.

## References

- 1 Y. Mai and A. Eisenberg, *Chem. Soc. Rev.*, 2012, **41**, 5969–5985.
- 2 N. J. Warren and S. P. Armes, *J. Am. Chem. Soc.*, 2014, **136**, 10174–10185.
- 3 F. Lv, Z. An and P. Wu, *Nat. Commun.*, 2019, **10**, 1397.
- 4 R. Momper, H. Zhang, S. Chen, H. Halim, E. Johannes, S. Yordanov, D. Braga, B. Blulle, D. Doblas, T. Kraus, M. Bonn, H. I. Wang and A. Riedinger, *Nano Lett.*, 2020, **20**, 4102–4110.
- 5 Q. Ye, M. Huo, M. Zeng, L. Liu, L. Peng, X. Wang and J. Yuan, *Macromolecules*, 2018, **51**, 3308–3314.
- 6 Z. Hua, J. R. Jones, M. Thomas, M. C. Arno, A. Souslov, T. R. Wilks and R. K. O'Reilly, *Nat. Commun.*, 2019, **10**, 5406.

- 7 H. Li, L. Han, Y. Zhu, P. Fernández-Trillo and F. He, *Macromolecules*, 2021, **54**, 5278–5285.
- 8 Z. J. Chen, S. C. Yang, X. L. Liu, Y. Gao, X. Dong, X. Lai, M. H. Zhu, H. Y. Feng, X. D. Zhu, Q. Lu, M. Zhao, H. Z. Chen, J. F. Lovell and C. Fang, *Nano Lett.*, 2020, **20**, 4177–4187.
- 9 G. Lin, J. Cai, Y. Sun, Y. Cui, Q. Liu, I. Manners and H. Qiu, *Angew. Chem., Int. Ed.*, 2021, **60**, 2–9.
- 10 H. Sun, Y. Hong, Y. Xi, Y. Zou, J. Gao and J. Du, *Biomacromolecules*, 2018, **19**, 1701–1720.
- 11 S. Varlas, R. Keogh, Y. Xie, S. L. Horswell, J. C. Foster and R. K. O'Reilly, *J. Am. Chem. Soc.*, 2019, **141**, 20234–20248.
- 12 Y. Liu, H. Wang, S. Li, C. Chen, L. Xu, P. Huang, F. Liu, Y. Su, M. Qi, C. Yu and Y. Zhou, *Nat. Commun.*, 2020, **11**, 1724.
- 13 Z. Lai, Q. Jian, G. Li, C. Shao, Y. Zhu, X. Yuan, H. Chen and A. Shan, *ACS Nano*, 2021, **15**, 15824–15840.
- 14 J. Li, L. Zeng, Z. Wang, H. Chen, S. Fang, J. Wang, C. Y. Cai, E. Xing, X. Liao, Z. W. Li, C. R. A. Jr, Z. S. Chen, H. Chao and Y. Pan, *Adv. Mater.*, 2021, **33**, e2100245.
- 15 G. Perli, Q. Wang, C. B. Braga, D. L. Bertuzzi, L. A. Fontana, M. C. P. Soares, J. Ruiz, J. D. Megiatto Jr., D. Astruc and C. Ornelas, *J. Am. Chem. Soc.*, 2021, **143**, 12948–12954.
- 16 W. Feng, G. Li, X. Kang, R. Wang, F. Liu, D. Zhao, H. Li, F. Bu, Y. Yu, T. F. Moriarty, Q. Ren and X. Wang, *Adv. Mater.*, 2022, **34**, e2109789.
- 17 W. Li, H. Palis, R. Merindol, J. Majimel, S. Ravaine and E. Duguet, *Chem. Soc. Rev.*, 2020, **49**, 1955–1976.
- 18 Y. Lu, J. Lin, L. Wang, L. Zhang and C. Cai, *Chem. Rev.*, 2020, **120**, 4111–4140.
- 19 R. Zeng, Z. Gong, L. Chen and Q. Yan, *ACS Macro Lett.*, 2020, **9**, 1102–1107.
- 20 J. Wan, B. Fan, K. Putera, J. Kim, M. M. Banaszak Holl and S. H. Thang, *ACS Nano*, 2021, **15**, 13721–13731.
- 21 B. Xu, H. Qian, L. Zhang and S. Lin, *Angew. Chem., Int. Ed.*, 2021, **60**, 17707–17713.
- 22 A. Nandakumar, Y. Ito and M. Ueda, *J. Am. Chem. Soc.*, 2020, **142**, 20994–21003.
- 23 S. Wang, M. C. Förster, K. Xue, F. Ehlers, B. Pang, L. B. Andreas, P. Vana and K. Zhang, *Angew. Chem., Int. Ed.*, 2021, **60**, 9712–9718.
- 24 J. Zhang, S. You, S. Yan, K. Muellen, W. Yang and M. Yin, *Chem. Commun.*, 2014, **50**, 7511–7513.
- 25 H. Sun and J. Du, *Macromolecules*, 2020, **53**, 11033–11039.
- 26 H. Sun, X. Li, K. Jin, X. Lai and J. Du, *Nanoscale Adv.*, 2022, **4**, 1422–1430.
- 27 Y. Sun, F. Gao, Y. Yao, H. Jin, X. Li and S. Lin, *ACS Macro Lett.*, 2021, **10**, 525–530.
- 28 Z.-Q. Wan, W.-M. Ren, S. Yang, M.-R. Li, G.-G. Gu and X.-B. Lu, *Angew. Chem., Int. Ed.*, 2019, **58**, 17636–17640.
- 29 D. Coban, O. Gridina, M. Karg and A. H. Gröschel, *Macromolecules*, 2022, **55**, 1354–1364.
- 30 Z. Zhao, X. Wang, X. Jing, Y. Zhao, K. Lan, W. Zhang, L. Duan, D. Guo, C. Wang, L. Peng, X. Zhang, Z. An, W. Li, Z. Nie, C. Fan and D. Zhao, *Adv. Mater.*, 2021, **33**, e2100820.
- 31 Y. Liu and H. Zhao, *Macromolecules*, 2021, **54**, 11412–11418.
- 32 D. Li, X. Chen, M. Zeng, J. Ji, Y. Wang, Z. Yang and J. Yuan, *Chem. Sci.*, 2020, **11**, 2855–2860.
- 33 H. Sun, S. Chen, X. Li, Y. Leng, X. Y. Zhou and J. Z. Du, *Nat. Commun.*, 2022, **13**, 2170.
- 34 I. C. Riegel, A. Eisenberg, C. L. Petzhold and D. Samios, *Langmuir*, 2002, **18**, 3358–3363.
- 35 X. Y. Liu, J. S. Kim, J. Wu and A. Eisenberg, *Macromolecules*, 2005, **38**, 6749–6751.
- 36 H. Sun, D. Liu and J. Du, *Chem. Sci.*, 2019, **10**, 657–664.
- 37 D. W. Van Krevelen and K. Te Nijenhuis, *Properties of Polymers: Their Correlation with Chemical Structure; Their Numerical Estimation and Prediction from Additive Group Contributions; Fourth, completely revised edition*, Elsevier, 2009, ch. 7, pp. 189–225.
- 38 G. Kacar, C. Atilgan and A. S. Ozen, *J. Phys. Chem. C*, 2010, **114**, 370–382.
- 39 C. E. Johnson, M. P. Gordon and D. S. Boucher, *J. Polym. Sci., Part B: Polym. Phys.*, 2015, **53**, 841–850.
- 40 X. Lyu, A. Xiao, W. Zhang, P. Hou, K. Gu, Z. Tang, H. Pan, F. Wu, Z. Shen and X.-H. Fan, *Angew. Chem., Int. Ed.*, 2018, **57**, 10132–10136.
- 41 Y. Hu, Y. Chen and J. Du, *Polym. Chem.*, 2019, **10**, 3020–3029.
- 42 J. Xiao and J. Du, *J. Am. Chem. Soc.*, 2020, **142**, 6569–6577.
- 43 Z. Huang, S. Chen, X. Lu and Q. Lu, *Chem. Commun.*, 2015, **51**, 8373–8376.
- 44 A. S. Ozen, U. Sen and C. Atilgan, *J. Chem. Phys.*, 2006, **124**, 064905.
- 45 N. E. Clay, J. J. Whittenberg, J. Leong, V. Kumar, J. Chen, I. Choi, E. Lias, J. M. Schieferstein, J. H. Jeong, D. H. Kim, Z. J. Zhang, P. J. A. Kenis, I. W. Kim and H. Kong, *Nanoscale*, 2017, **9**, 5194–5204.
- 46 S. Lin, H. Sun, E. J. Cornel, J.-H. Jiang, Y.-Q. Zhu, Z. Fan and J.-Z. Du, *Chin. J. Polym. Sci.*, 2021, **39**, 1538–1549.
- 47 H. Sun, X. Zhou, Y. Leng, X. Li and J. Du, *Macromol. Rapid Commun.*, 2022, **43**, 2200131.
- 48 L. S. Li, H. Jiang, B. W. Messmore, S. R. Bull and S. I. Stupp, *Angew. Chem., Int. Ed.*, 2007, **46**, 5873–5876.
- 49 Y. Wang, W. Qi, R. Huang, X. Yang, M. Wang, R. Su and Z. He, *J. Am. Chem. Soc.*, 2015, **137**, 7869–7880.